



HAL
open science

Early detection and diagnosis of thermal runaway reactions using model-based approaches in batch reactors

Amine Dakkoune, Lamiae Vernières-Hassimi, Dimitri Lefebvre, Lionel Estel

► **To cite this version:**

Amine Dakkoune, Lamiae Vernières-Hassimi, Dimitri Lefebvre, Lionel Estel. Early detection and diagnosis of thermal runaway reactions using model-based approaches in batch reactors. *Computers & Chemical Engineering*, 2020, 140, pp.106908 -. 10.1016/j.compchemeng.2020.106908 . hal-03490291

HAL Id: hal-03490291

<https://hal.science/hal-03490291>

Submitted on 22 Aug 2022

HAL is a multi-disciplinary open access archive for the deposit and dissemination of scientific research documents, whether they are published or not. The documents may come from teaching and research institutions in France or abroad, or from public or private research centers.

L'archive ouverte pluridisciplinaire **HAL**, est destinée au dépôt et à la diffusion de documents scientifiques de niveau recherche, publiés ou non, émanant des établissements d'enseignement et de recherche français ou étrangers, des laboratoires publics ou privés.



Distributed under a Creative Commons Attribution - NonCommercial 4.0 International License

Early detection and diagnosis of thermal runaway reactions using model-based approaches in batch reactors

Amine Dakkoun^{1,2}, Lamiae Vernières - Hassimi¹, Dimitri Lefebvre², Lionel Estel¹

¹Normandie Université, INSA Rouen, UNIROUEN, LSPC, EA4704, 76000 Rouen, France,

²Université Le Havre Normandie – GREAH, 25 rue P. Lebon, 76063 Le Havre, France.

E-mail : amine.dakkoun@insa-rouen.fr

Abstract

Since the early 1990s, considerable efforts have been made in researching and applying approaches for faults detection and diagnosis in chemical processes. The occurrence of chemical accidental events due to thermal runaways have serious consequences for the human, environmental and economic and encourage these efforts. This is the main motivation for this paper that details a fault detection and diagnosis approach for exothermic reactions. The proposed approach is based on the temperature measurements. It compares the collected measurements with a reference behaviour for early thermal runaway detection. Once a fault is detected, characteristic features are extracted from the successive measurements collected within a time window. The fault isolation is based on a classification of these features with respect to several faulty modes. The studied faults are the most responsible for thermal runaway events. A multiset of linear classifiers and binary decision diagrams indexed with respect to the time are used for that purpose. The synthesis of peroxyformic acid in a batch reactor is considered to validate the proposed method by numerical simulations and experiments. The performance of the proposed method is carried out in a systematic way in order to evaluate its robustness and efficiency.

Keywords: Fault detection; fault isolation; thresholds; parameters characteristics; batch reactor; thermal runaway.

1. Introduction

Since the last decades, a growing demand for reliability and safety of chemical processes has been requested (Francis and Bekera, 2014; Jain et al., 2019, 2018). This requirement results from the progressive development of the chemical industries making the systems more and

more complex to control and the increasing number of chemical accidental events leaving serious consequences for the humans, the environment and the economy. In many chemical industrial sectors, in particular in the fine chemical industries, most synthetic reactions are exothermic. The major problem with these reactions is the loss of temperature control in the case of malfunctions. In this situation, a thermal runaway event can occur (Westerterp and Molga, 2006). According to a study conducted by our group (Dakkoune et al., 2018a; Dakkoune et al., 2019), 25% of chemical events in France are due to thermal runaways. Balasubramanian and Louvar (2002) has also proved that 26% of the chemical events in the United States are due to the same phenomena.

Thermal runaways is a phenomenon that takes place during an exothermic reaction. The reaction produces heat that contributes to the increase in temperature and accelerates the speed of the reaction. Then again, this will lead to a higher production of heat that in turn causes a further increase in the temperature of the reaction, and so on. As long as the heat released by the reaction is less than the heat released by the reactor cooling system, the chemical system is considered to be controlled. In the case where the heat dissipated is less than the heat given by the reaction, this can lead to a thermal runaway; this mechanism has been described by different authors (Semenov, 1928; Stoessel, 2008). This phenomenon can happen also when the temperature of the reaction medium exceeds a certain threshold, secondary reactions can be triggered, in particular the decomposition reactions which are generally exothermic. Consequently, the cooling system can become undersized in relation to these secondary reactions. For this reason, it is necessary to monitor the temperature profile of the reaction medium in order to maintain the system below this threshold (Vernieres-Hassimi et al., 2015).

Industrial demand requires working under operating conditions in a safe zone of the reactor. However, the reactor is never sheltered from a technical failure or human error, which may lead to operation in an unsafe area for the reactor. The method proposed in this article allows to detect a malfunction and to isolate the fault in order to have a better understanding of the thermal runaway situations. It is the first step either to stop the installation or to correct the error if it is technically possible.

In this context, maintaining safe operating conditions for chemical reactors is a primordial necessity. From the beginning of the 1990s, the research effort intensified to focus on monitoring approaches (Miljković, 2011). The purpose was to ensure and maintain a reliable

level of safety in chemical reactors, to minimize the risk of thermal runaways and prevent abnormal faults progression. The purpose of monitoring is to alert and inform the user of the appearance of faults so that they can react as quickly as possible. The monitoring is divided into two complementary functions:

- Fault detection that generates alarms in order to signal the occurrence of the faults.
- Fault diagnosis that identifies the nature of the detected faults. This function includes the isolation step that determine the most probable fault among a set of fault candidates.

Fault detection and diagnosis can be carried out with different methods that have some common characteristics. On one hand, the detection is performed by comparing the output signals of the system under normal and abnormal conditions in order to generate residuals. The evaluation of these residuals is performed thanks to thresholds and decision functions (Frank and Ding, 1997). On the other hand, the fault diagnosis is based on an extraction of characteristic features from the sensor measurements. These features are used to classify the signals into a set of predetermined classes.

In this present work, a fault detection and diagnosis method was developed for exothermic reactions that may experience thermal runaway events due to some faults that result mainly from operator errors (Dakkoune et al., 2018a; Dakkoune et al., 2019; Saada et al., 2015). The particular reaction that leads to the synthesis of peroxyformic acid from formic acid and hydrogen peroxide is studied. Six classes of fault were considered related on one hand to unacceptable errors in the initial conditions and on the other hand to the presence of impurities or to failures of the stirrer or heat transfer system. The detection method compares the actual temperature measurements with a reference behaviour obtained with a precise model of the reaction. A double dynamical threshold is introduced for that purpose.

The innovation of the proposed approach lies on several aspects. Indeed, the approach is characterized by its generality, it can adapt to simple or complex chemical systems that may be linear or nonlinear. This functionality is found in few approaches like the Parity approach space and Fuzzy logic. The ease of processing and interpreting system data and the simplicity of the application are also a strong point of this approach. In addition, the proposed approach is well suited to any fault, as long as this fault affects the thermal behavior of the reaction. In fact, monitoring by a unique measured signal (here the reaction temperature) is sufficient to carry out online fault detection and diagnosis and in real time. On the other side, the

originality of the proposed approach relies also on the use of dynamic thresholds to carry out rapid fault detection, as well as the use of several statistical characteristics to separate the collected measurements for diagnosis issue.

In particular, this model includes an additional decomposition mode that explains the temperature variation due the presence of impurities as copper sulfate (Vernières-Hassimi et al., 2017). The model also explained the effects of the stirrer and of the heat transfer flow. Then, the isolation is obtained according to a classification method of the essential features extracted from the temperature variation within a sliding window. This classification combines linear separators and binary decision diagrams that are useful to isolate the six possible faults. The innovation of the approach is to use off-line the numerical model to emulate each fault at different times and to design a database of degraded behaviours. The set of linear separators and binary decision diagrams, indexed by time, is computed from this database.

The paper is organized as follows. Section 2 is about the state of the art. Section 3 describes the considered reaction and the experimental device. Section 4 is about the data pre-processing. Then, Section 5 describes the main contributions and details the detection and diagnosis method. Section 6 is about the numerical and experimental results. Section 7 gives the conclusions and perspectives of the study.

2. Literature survey

There exists huge amount of contributions about fault detections and diagnosis and also many ways to present these different methods. One can for example, separate the approaches in model-based, data-based and knowledge-based approaches.

First, model-based approaches are based on the design of residual signals that are near zero in the normal case and significantly different from zero in abnormal situations (Frank, 1990)(Gertler and Singer, 1990). Parity space use projections of the measurements in an adequate subspace (Kabbaj et al., 2009; Gertler and Singer, 1990). State observers aim to reconstruct the system state in order to evaluate the difference between the measured outputs and their estimates (Benkouider et al., 2009; Frank, 1990; Pierri et al., 2008). Parameter estimation methods track some parameters of interest with identification approaches (Fadda et al., 2019; Isermann, 2006; Kabbaj et al., 2009). Qualitative methods also exist mainly based on cause-and-effect diagrams (Olivier-Maget et al., 2009).

Then, data-based approaches are based on process measurements or history. Control charts and tests for change detection have been used from more than 50 years in many application domains (Basseville and Nikiforov, 1993). In particular X control chart is popular in chemical engineering for a long time (Bryce et al., 1997). Note that the EWMA control chart introduced by Roberts (1959), the CUSUM control chart proposed by Page (1954) or more recently the non-central chi-square chart proposed by Costa and Rahim (2006) can also be used. Principal component analysis (PCA) is another data-based approach that detects the presence of a fault by measuring the effect of this fault in the correlation between the variables (Alcala et al., 2012; Bin Shams et al., 2011; Du and Du, 2018; Lee et al., 2004; Miljković, 2011). In the case of nonlinear systems - the case of most chemical reactions - an extension of the Kernel PCA method (KPCA) can be used (Fezai et al., 2018; Harkat et al., 2019; Jia et al., 2000). Neural networks are another tool used for detection and isolation (Othman et al., 2012; Zhao, 2018), (Benkouider et al., 2012; Zhang, 2008).

Finally, knowledge-based methods include expert systems that take the best decision by expert domain operators, according to the knowledge obtained from the history in the field (Cilliers, 2013; Di Maio et al., 2018; Rich et al., 1989). The extraction, representation, and coding of the knowledge lead to the faults isolation (Quantrille and Liu, 2012; Ramesh et al., 1992). Fuzzy logic is another tool for integrating knowledge into algorithms, in order to compute decisions about the possible occurrence of faults (Ammiche et al., 2018; Ballesteros-Moncada et al., 2015; Kohcielny, 1999). Finally, qualitative trend analysis represents the trend of signals in normal and abnormal cases, in order to get a global vision on the process behaviour and to distinguish anomalies (Thürlimann and Villez, 2017; Zhou and Ye, 2016).

When focusing on thermal runaway, one should first notice that this issue may appear in a large variety of reactions, in particular in many battery systems due to the stress, posing a major threat to the overall safety of such systems (Liao et al., 2019). Thermal runaway mainly occurs due to the domino effect (Feng et al., 2016; Lamb et al., 2015; Ouyang et al., 2018; Smith et al., 2010; Walker et al., 2019). There exist basically three types of thermal runaway monitoring and detection schemes: using the terminal voltage and the surface temperature (Liu et al., 2019; Misyris et al., 2019; Xiong et al., 2018); using the internal temperature (Fortier et al., 2017; Ganguli et al., 2017; Raghavan et al., 2017; Raijmakers et al., 2019), tracking the characteristic vent gas component during thermal runaway (Fernandes et al., 2018; Koch et al., 2018).

Thermal runaway may appear also in other chemical industries and several criteria for predicting the thermal runaway onset in batch and semi-batch reactors have been suggested for such issues. Semenov criterion (Semenov, 1928) allows the thermal runaway prediction based on the thermal power produced and evacuated by the system. According to this criterion, a detection of the runaway limit is reached when the reaction power becomes dominant. However, this criterion does not take into account reagents consumption during the reaction.

To overcome this limit, other criteria based on the second derivative of the reaction temperature over time (Adler and Enig, 1964) and the second derivative of the reaction temperature over its conversion (Bowes, 1984) have been developed. In these cases, thermal runaway occurs when one of these dimensionless derivatives becomes positive before the temperature hotspot. However, these criteria do not give any measure of thermal runaway intensity.

For this reason, other criteria are developed as the Hub and Jones (1986) criterion, which indicates that the runaway occurs when the first and second derivatives of the reactor temperature are both positive. The divergence criterion of Strozzi and Zaldívar (1994) shows that if the system of differential equations that describes the process presents a positive divergence at a certain point on the temperature profile, the process works in runaway conditions. These criteria do not require any detailed information on the process but on the other hand, these criteria are highly sensitive to the presence of noise.

More recently, Strozzi et al. (1999) have developed a new method based on the extraction of information on the behavior of the reactor by phase-space reconstruction, using the time delay embedding of the temperature measurements. Detection is based on dramatic changes in the behavior of space-phase trajectories. Based on the work of Strozzi et al. (1999), Bosch et al. (2004) used pressure measurements instead of temperature. The results show that the pressure provided early detection of runaway initiation. However, temperature leads to an earlier detection. Marco et al. (1997) have also tested monitoring of the gas phase composition using mass spectrometry. The results found show earlier detection compared to methods based on temperature measurements. These studies show that fault detection and diagnosis can be carried out with several parameters, like pressure, temperature, concentration, etc. However, the detection rapidity depends on the measured parameter, in fact, the concentration

measurement allowed to achieve the fastest detection of thermal runaway, followed by temperature and finally pressure. However, the concentration measurement in real time is more complicated and more expensive; therefore, most of the detection methods are based on the temperature measurement of the reaction medium.

In their article, Subramanian et al. (2014) proposed a method based on statistical learning theory to estimate the reactor heat release under normal and defective conditions. The faults detection is carried out according to the residue obtained and the faults classification is carried out from the extracted image characteristics. Benkouider et al. (2012) have proposed another method based on the reaction model, and the use of extended Kalman filter to estimate the reactor state through the overall heat transfer coefficient. Fault detection is based on the statistical test and fault diagnosis is based on a probabilistic neural network classifier.

In this work, the maximum reaction temperature (T_{max}) was our criterion for the development of the detection and diagnosis method. The maximum temperature variation in an exothermic reaction is a key parameter in the safety of chemical reactors (Chetouani et al., 2003; Vernières-Hassimi et al., 2015), because when this temperature exceeds a specific limit, dangerous decomposition reactions can be triggered. The maximum reaction temperature can be modified in the presence of defects. Monitoring of this parameter resulting from the exothermicity of the chemical reaction makes it possible to avoid the occurrence of runaway reactions (Vernières-Hassimi et al., 2012). Indeed, the proposed approach can be overcome several limits cited above. In addition to its ability to adapt to any chemical system and any defect with ease of processing and interpretation of system data.

3. Problem statement

The considered problem is to detect and isolate faults that may occur during exothermic reactions in a batch reactor RC1 under isoperibolic conditions. A new method that combines a data-based approach and a numerical model of the reaction will be used for this purpose.

3.1. Experimental device

The experimental device is composed by the calorimeter reactor RC1 (Figure 1). The RC1 calorimeter is an automated reactor used to measure thermal profiles during a chemical reaction. The main installation includes a jacketed reactor equipped with an agitator shaft, a

temperature probe, a calibration probe in order to measure the overall heat exchange coefficient, and a condenser that avoids the evaporation of liquid phase compounds. The reactor is operating in batch mode.

The stirred tank is made of glass with a capacity of two liters and equipped with a glass jacket. A rapid passage of the heat transfer fluid (the silicone oil 47 V 20) with a fixed flow rate of $1.33 \text{ kg}\cdot\text{s}^{-1}$ allows to keep an uniform temperature in the double jacket. The mechanical stirrer has a variable speed from 30 to 850 rpm. The sensor measures every two seconds the temperature of the reaction T_r and the temperature of the heat transfer fluid T_j thanks to platinum probes Pt100. The installation is connected with the WinRC NT software for online data acquisition.

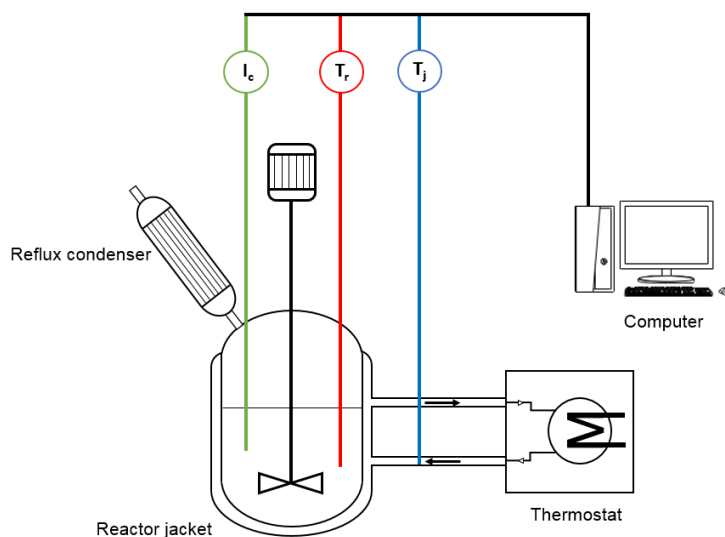


Figure 1. Schematic representation of the RC1 pilot reactor.

3.2. Perhydrolysis of formic acid reaction

Peroxyformic acid (PFA) is a strong oxidant that respects the environment thanks to its green synthesis (Filippis et al., 2009). PFA is used in many chemical treatments as bleaching (Sun et al., 2011) or epoxidation of unsaturated oils to produce biofuels (Campanella et al., 2008; Wang et al., 1997). It is also a disinfectant and food preservative used in the medical and food industries (Sun et al., 2011). However, a safety assessment showed that PFA synthesis presents a risk of class 5 (high risk) according to the Stoessel classification (Leveneur et al., 2012). The unstable state of PFA makes it unsafe and able to trigger immediately a

decomposition reaction in the case of loss control of the reaction (Stoessel, 2008) that may result in a thermal runaway. This motivates our study about early detection and fault diagnosis for PFA synthesis.

More precisely, the synthesis of PFA from formic acid (FA) and hydrogen peroxide (HP) is studied by RC1 reactor in a batch mode and under isoperibolic mode of temperature (Zheng et al. 2016). The reaction is controlled by the heating / cooling system. A titration method is applied to determine the initial concentration of reagents. A standard solution of ammonium cerium sulfate (0.1 mol.L^{-1}) and a standard solution of sodium hydroxide (0.4 mol.L^{-1}) are used as a titrant to determine the initial concentration of hydrogen peroxide and formic acid respectively. The normal operating conditions of this reaction are given in Table 1.

Table 1. Normal operating conditions of the reaction at initial time

System Parameter	Symbol	Value	Unit
Sample volume	V_r	1.2	L
Initial concentration of formic acid	$[FA]$	2.5	mol.L^{-1}
Initial concentration of hydrogen peroxide	$[HP]$	2.8	mol.L^{-1}
Initial temperature of reaction	T_r	70	$^{\circ}\text{C}$
Temperature of the heat transfer fluid	T_j	70	$^{\circ}\text{C}$
Stirring rate	N_{tr}	400	rpm

The whole reaction is composed by the perhydrolysis of FA, the two ways of decomposition of PFA and the decomposition of HP according to Figure 2. The heat increases due to these reactions.

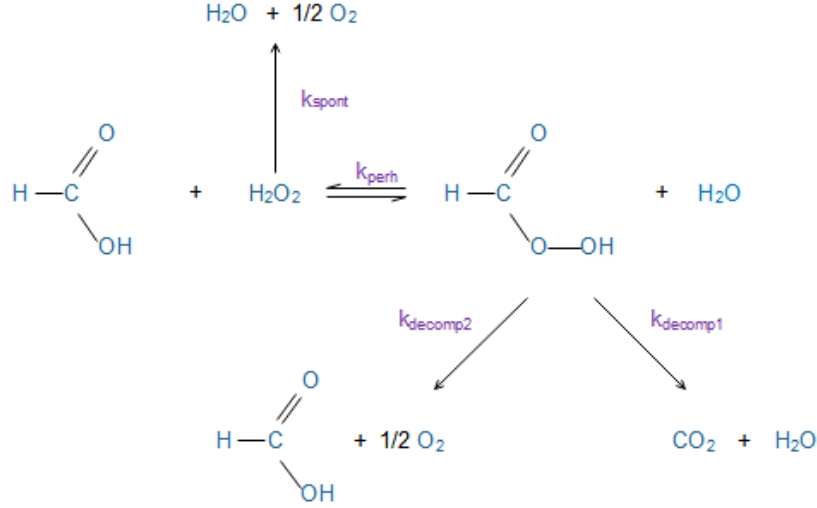


Figure 2. Simplified mechanism for the perhydrolysis of formic acid reaction.

3.3. Kinetics, mass and energy balances

The kinetic equations are detailed for each reaction of the system (Figure 2). Let us first define $k_{0,y}$ as the pre-exponential factor and $E_{a,y}$ as the activation energy of the reaction y for $y \in \{perh, decomp1, decomp2, spont, cat\}$. R is a gaz constant, T_r is the reaction temperature and T_{ref} is the reference temperature. K_{FAD}^C is the association parameter of formic acid and K^C is the equilibrium parameter of the perhydrolysis reaction. $[x]$ denotes the concentration of the chemical compound $x \in \{HCOOH, H_2O_2, HCOOH, H_2O\}$.

A first reaction results from the perhydrolysis of formic acid reaction, Eq. (1) (Zheng et al., 2016).

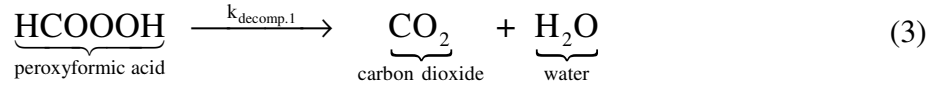


The kinetic expression of this reaction is given by Eq. (2):

$$R_{perh} = k_{0,perh} \exp\left(\frac{-E_{a,perh}}{R} \left(\frac{1}{T_r} - \frac{1}{T_{ref}}\right)\right) \sqrt{K_{FAD}^C \frac{HCOOH}{H_2O}} \left([HCOOH][H_2O_2] - \frac{1}{K^C} [HCOOOH][H_2O] \right) \quad (2)$$

where K_{FAD}^C is the parameter of association of the formic acid and K^C the equilibrium parameter of the perhydrolysis reaction.

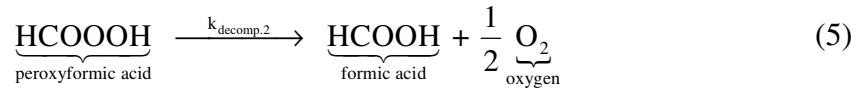
The second reaction results from the decomposition of peroxyformic acid into CO₂ and H₂O, Eq. (3).



The kinetic expression of this reaction is given in Eq. (4):

$$R_{\text{decomp1}} = k_{0,\text{decomp1}} \exp\left(\frac{-E_{a,\text{decomp1}}}{R} \left(\frac{1}{T_r} - \frac{1}{T_{\text{ref}}}\right)\right) [\text{HCOOOH}] \quad (4)$$

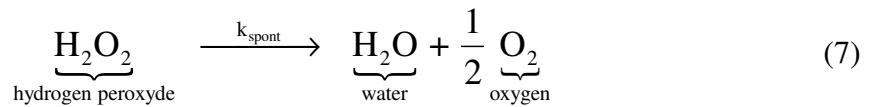
The third reaction results from the decomposition of peroxyformic acid into formic acid and oxygen, Eq. (5).



The kinetic expression of this reaction is given in Eq. (6):

$$R_{\text{decomp2}} = k_{0,\text{decomp2}} \exp\left(\frac{-E_{a,\text{decomp2}}}{R} \left(\frac{1}{T_r} - \frac{1}{T_{\text{ref}}}\right)\right) [\text{HCOOOH}] \quad (6)$$

The fourth reaction results from the decomposition of hydrogen peroxide into water and oxygen, Eq. (7). Hydrogen peroxide also decomposes spontaneously under the effect of the heat. The kinetics of the reaction and the reaction mechanism was developed by Vernières-Hassimi et al. (2017).



The kinetic expression of this reaction is given in Eq. (8):

$$R_{\text{spont}} = k_{0,\text{spont}} \exp\left(\frac{-E_{a,\text{spont}}}{R} \left(\frac{1}{T_r} - \frac{1}{T_{\text{ref}}}\right)\right) [\text{H}_2\text{O}_2] \quad (8)$$

Table 2. Values of kinetic and thermodynamic parameters for $T_{ref} = 67 \text{ }^\circ\text{C}$ (Eq. (2), Eq. (4) and Eq. (6)) (Zheng et al., 2016), and for $T_{ref} = 140 \text{ }^\circ\text{C}$ (Eq. (8)) (Vernières-Hassimi et al., 2017).

Kinetic and thermodynamic parameters	Value	Unit
$k_{0,perh}$	0.15	$\text{L.mol}^{-1}.\text{s}^{-1}$
$E_{a,perh}$	150000	J.mol^{-1}
$\Delta H_{r,perh}$	- 5580	J.mol^{-1}
$k_{0,decomp1}$	0.001	s^{-1}
$E_{a,decomp1}$	20000	J.mol^{-1}
$\Delta H_{r,decomp1}$	- 359000	J.mol^{-1}
$k_{0,decomp2}$	0.0009	s^{-1}
$E_{a,decomp2}$	20200	J.mol^{-1}
$\Delta H_{r,decomp2}$	- 163000	J.mol^{-1}
$k_{0,spont}$	0.0000924	s^{-1}
$E_{a,spont}$	150000	J.mol^{-1}
$\Delta H_{r,spont}$	- 98000	J.mol^{-1}

The mass balance for FA, HP, PFA and H_2O in a batch reactor are represented by Eq. (9):

$$\begin{aligned} \frac{dC_{HCOOH}}{dt} &= -R_{perh} + R_{decomp2} \quad ; \quad \frac{dC_{HCOOOH}}{dt} = R_{perh} - R_{decomp2} - R_{decomp1} \\ \frac{dC_{H_2O_2}}{dt} &= -R_{perh} - R_{decomp3} \quad ; \quad \frac{dC_{H_2O}}{dt} = R_{perh} + R_{decomp1} + R_{decomp3} \end{aligned} \quad (9)$$

The energy balance in the batch reactor is expressed by Eq. (10):

$$\frac{dT_r}{dt} = \frac{1}{\sum m_r C_{Pr}} \left(UA.(T_j - T_r) - \sum R_r \cdot \Delta H_{r,y} \cdot V_r - q_{loss} \right) \quad (10)$$

where m_r is the initial mass of the reaction mixture. C_{Pr} is the heat capacity of the reaction mixture. U is the overall heat-transfer coefficient. A is the heat transfer area. T_j is the heat carrier temperature circulating in the reactor jacket. R_r is the reaction rate. $\Delta H_{r,y}$ is the enthalpy of the reaction y . V_r is the volume of the reaction mixture. q_{loss} is the heat loss due to evaporation.

According to Ubrich et al., (2001), the heat losses in the reaction are mainly due to the evaporation of the reaction mixture and the heat exchanges with the jacket. It is assumed that heat losses are proportional to the total vapor pressure, Eq. (11).

$$q_{loss} = \beta \sum x_j P_j \quad (11)$$

where β is a constant, x_j is the molar fraction of component j and P_j is the vapor pressure of component j . According to Zheng et al. (2016), the β coefficient was fixed at 34.54 J/MPa, and the vapor pressure can be estimated using the Clausius - Clapeyron equation.

$$P(T_1) = P(T_2) \exp\left(\frac{\Delta H_V}{R} \left(\frac{1}{T_1} - \frac{1}{T_2}\right)\right) \quad (12)$$

where ΔH_V is the heat of vaporization, $P(T_1)$ and $P(T_2)$ are the vapour pressures at temperatures T_1 and T_2 respectively. Since water and formic acid are the most volatile compounds, only their evaporation has been taken into account.

3.4. Numerical model

The previous model is used to simulate the thermal behaviour of the system. The numerical simulation and the experimental measurements of the temperature variations in batch reactor are reported in Figures 3 and 4 under normal operating conditions (Table 1). For the sake of clarity, all the numerical points have been presented on Figures 3 and 4 (curves), however, only a few experimental points have been chosen to be recognized on Figures 3 and 4 (x-plot). Note that the temperature reaches a maximal value after 35 min under normal operating conditions and then starts to decrease. The results in Figure 4 show a correct estimate of the experimental thermal behavior of the reaction by the numerical model during the first phase of the reactions (i.e. within time interval [0, 35min]). It should be noted that this first phase of the reaction which is used for the detection of faults. This maximal value will be used next in order to define dynamical detection thresholds.

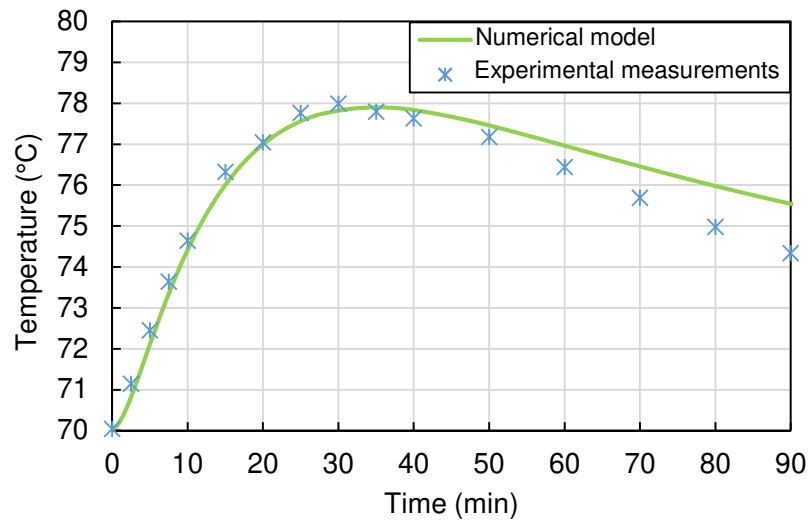


Figure 3. Simulated and experimental mixture temperature (T_r) profiles

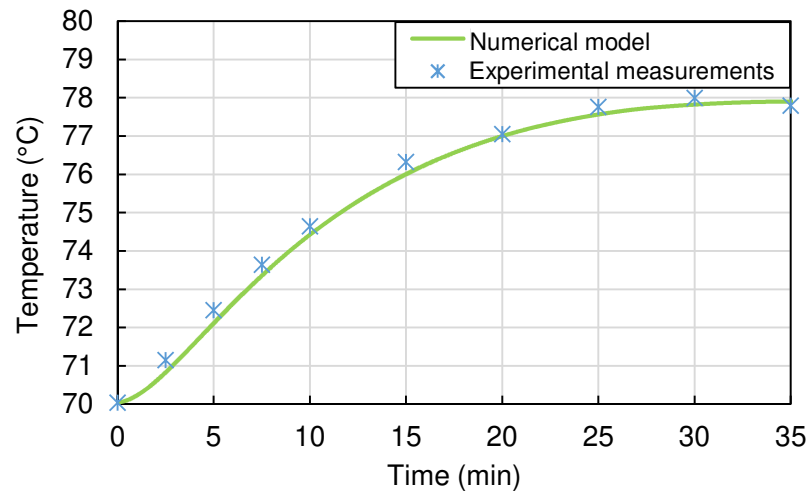


Figure 4. Mixture temperature (T_r) profiles within time interval [0, 35min].

3.5. Defects

Faults may affect the parameters of normal operating conditions. The dysfunctional scenarios selected in this study are based on operator errors (Dakkoune et al., 2018a; Saada et al., 2015). They are the most frequent in the chemical industry and may lead to thermal runaway scenarios.

Six classes of faults were considered in this work. These faults are divided into two types (Table 3):

- Type 0 faults are related to the reagent initial concentration and to the possible presence of impurities. They occur only at initial time.

- Type 1 faults may occur at any time because they are related to the actuators used to keep the system under control. These faults can occur in the initial time of reaction because of operating conditions or during the reaction due to changes in process measurements by control systems or technical defect.

Table 3. Description of the considered faults.

Fault type	Fault Number	Symbol	Description
0	F1	δFA	Increase in the initial concentration of formic acid.
	F2	δHP	Increase in the initial concentration of hydrogen peroxide.
	F3	δCu	Presence of impurities (metals such as copper sulfate).
1	F4	δT_j	Increase in the temperature of the heat transfer fluid.
	F5	δN_{tr}	Decrease in the stirring rate.
	F6	δQ_m	Decrease in the flow of heat transfer fluid.

Faults 1 and 2 represent an increase in the initial concentrations of reagents (formic acid and hydrogen peroxide) caused by the operator in the preparation step. The presence of these two faults in the reaction system with the magnitude shown in Table 6, has an effects on the thermal behavior of the reactor. An increase in the initial concentrations of the reagents generates an increase in the speed of the reactions. The heat balance expressed as a function of the thermal power released by the reaction (Eq. (10)) will lead to an increase in the maximum temperature of the reaction.

Fault 3 may appear in the case of the presence of small amounts of impurities (as copper sulfate, for example) due to insufficient cleaning of the reactor when the reactor is reused after another reaction, 7% of thermal runaways events in France are caused by the impurities remaining in reactors (Dakkoune et al., 2019). The presence of the copper sulfate (even in ppm quantities, see Table 6) may accelerate the kinetics of the decomposition of hydrogen peroxide in low temperature ranges. In this case, the kinetic expression of reaction Eq. (8) should be replaced by Eqs. (13) and (14). The kinetic equation of the HP decomposition catalyzed by the Cu^{2+} ions (Eq. (14)) becomes more complex (Perez-Benito, 2001). The heat balance (Eq. (10)) that is expressed as a function of the different kinetic equations will in turn cause an increase in the maximum temperature reached, according to Eq. (14) and Table 4 (Vernières-Hassimi et al., 2017).

$$R_{decomp3} = R_{spont} + R_{Cat} \quad (13)$$

$$R_{Cat} = 2k_{0,A} \exp\left(\frac{-E_{a,A}}{R} \left(\frac{1}{T_r} - \frac{1}{T_{ref}}\right)\right) [Cu^{2+}] [H_2O_2]^2 + 2k_{0,B} \exp\left(\frac{-E_{a,B}}{R} \left(\frac{1}{T_r} - \frac{1}{T_{ref}}\right)\right) [Cu^{2+}]^{1/2} [H_2O_2] \quad (14)$$

Table 4. Values of kinetic and thermodynamic parameters of Eq. (14) with $T_{ref} = 140^\circ\text{C}$ (Vernières-Hassimi et al., 2017).

Kinetic and thermodynamic parameters	Value	Unit
$k_{0,A}$	0.0163	$\text{L}^2 \cdot \text{mol}^{-2} \cdot \text{s}^{-1}$
$E_{a,A}$	162000	$\text{J} \cdot \text{mol}^{-1}$
$k_{0,B}$	0.0035	$\text{L}^2 \cdot \text{mol}^{-2} \cdot \text{s}^{-1}$
$E_{a,B}$	69700	$\text{J} \cdot \text{mol}^{-1}$
$\Delta H_{r,cat}$	- 93200	$\text{J} \cdot \text{mol}^{-1}$

Fault 4 represents an increase of the temperature of the heat transfer fluid from a faults magnitude shown in Table 6, due to a non-compliance with safety instructions by the operator. The non-compliance in this case is manifested by an overshoot of the nominal jacket temperature, which is fixed in the safety procedures equal to 70°C . This fault acts on the heat exchanged through the reactor jacket. Thereafter, the heat balance (Eq. (10)) will increase the reaction temperature.

Faults 5 and 6 cause a significant change in the overall heat exchange coefficient U due to a decrease in the stirring rate δN_{tr} or in the flow of the heat transfer fluid δQ_m , from a faults magnitude shown in Table 6. The explicit impact of δN_{tr} and δQ_m is not detailed in this paper but can be found in (Dream, 1999, Trambouze and Euzen, 2002). The presence of these faults acts directly on the quantity of heat exchanged with the reactor, and consequently on the thermal balance of reaction expressed according to Eq. (10).

The described faults have been simulated and validated experimentally. Figure 5 represents the experimental validation and the numerical simulations of the temperature reaction variation under normal and abnormal conditions after filtered by Kalman filter (except fault δQ_m that was not validated for safety reasons). In the next section, a fault detection and diagnosis approach is proposed through the online acquisition of the temperature measurements.

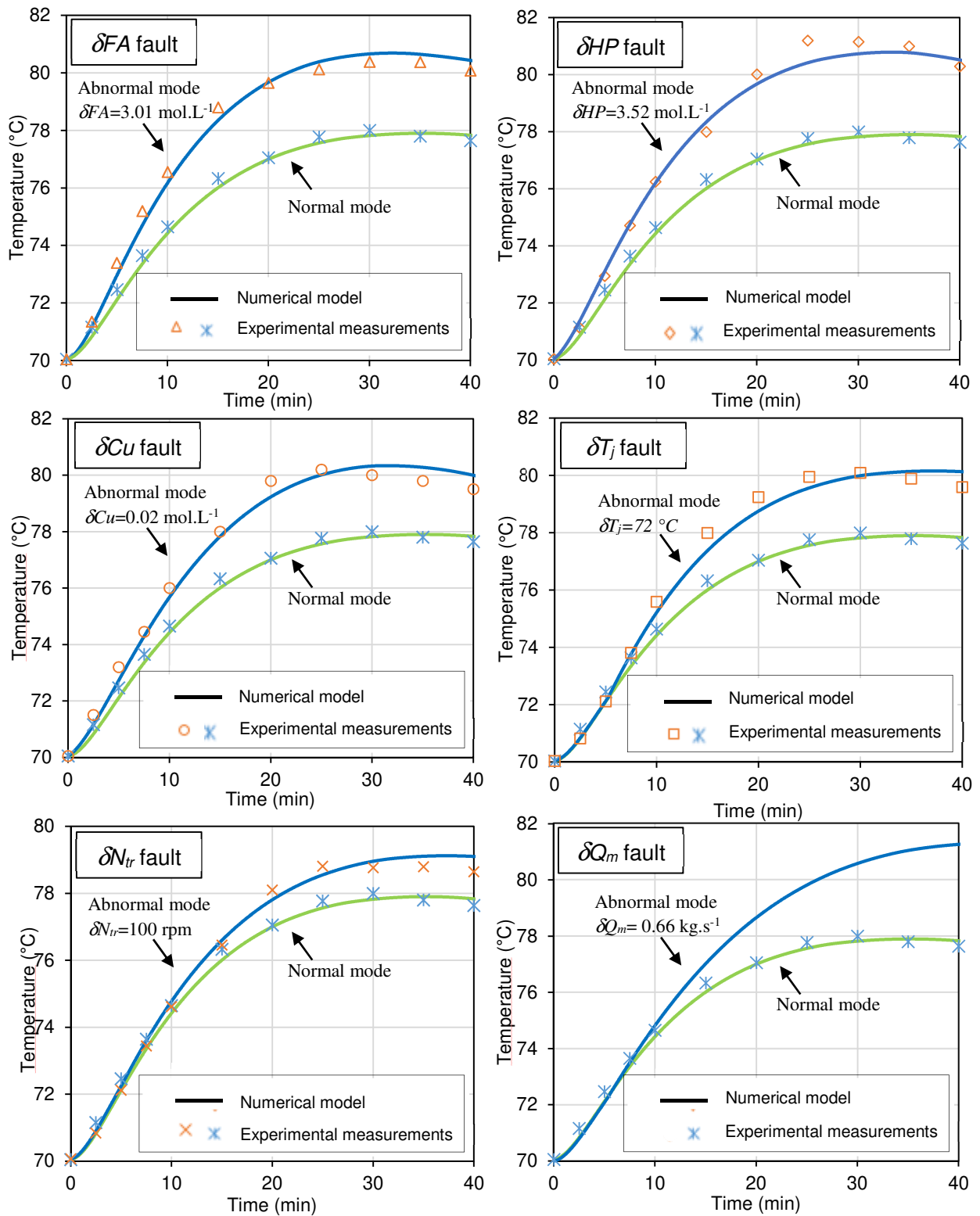


Figure 5. Experimental validation and numerical simulations of the temperature reaction variation under normal and abnormal conditions.

4. Data pre-processing

4.1. Sensoring

The variation of temperature T_r in an exothermic reaction is a key parameter for the safety of chemical reactors (Vernieres-Hassimi et al., 2015). Indeed, the maximum temperature of the reaction changes if faults infect the reactions leading to the occurrence of secondary reactions. The monitoring of T_r may avoid thermal runaways as long as the abnormal temperature variations are early detected. The RC1 reactor is equipped with a Pt100 sensor that measures the temperature every two seconds with a tolerance of 0.08 °C. In Pt100 sensor, the measurement is based on the variation of the resistance of platinum under the influence of the temperature. This sensor is the most frequently used for industrial applications, because of its advantages such as a wide temperature range from -200 °C up to 850 °C and a high precision and sensitivity.

4.2. Noise reduction

First, a Kalman filter is used to reduce the measurement noise. The efficiency of Kalman filter has been proved in numerous industrial applications (Jazwinski, 1970, Gelb, 1974). The Kalman filter is a recursive estimator that estimates the current state of the system from a single estimate of the previous state and the current measurements. In the case of linear systems, the Kalman filter relies on a two-step process: prediction and scraping. The scraping corrects the prediction of the system state by considering the estimate of the previous state. For more details, one can refer to (Chen and Chui, 1991).

4.3. Margin of tolerance M_T and memory parameter n

In the first minutes of the reaction, abnormal and normal behaviours are close. Because of the residual noise, false alarms may occur during this period. To overcome this problem, two parameters are introduced:

- The margin of tolerance M_T eliminates false alarms at the beginning of the reaction by ignoring all suspect variations with magnitude less than M_T .
- The memory parameter n also contributes to eliminate some false alarms. An alarm is only triggered when T_r exceeds the detection threshold for n consecutive acquisitions.

Based on our previous study on the same system (Dakkoune et al., 2018b), it was proved that M_T and n parameters have a major influence on the detection performance. Selecting $M_T = 0.05$ and $n = 10$ significantly reduces the false alarm rate, keeping reasonable values of the detection delay and non-detection rate.

4.4. Features extraction

Values of T_r are collected within a time window W . Then, first and second derivatives of T_r are computed and several statistical features are extracted (Table 5).

Table 5. The three types of statistical features.

Types of statistical features		
Position measurements	Dispersion measurements	Shape measurements
Mean	Variance	Skewness
Mode	Covariance	Kurtosis
Median	Standard deviation	

From an exhaustive study on these statistical characteristics based on the principal component analysis, the variance and skewness of the temperature have been proved to be the most representative parameters for faults detection and diagnosis (according to the considered faults) (Dakkoune et al., 2018b).

5. Detection and diagnosis method

5.1. Safe, dangerous and critical modes

For detection issues, the temperature profile will be divided in several areas. The detection method is based on the computation of two dynamical thresholds $D_{Limit}(t)$ and $S_{Limit}(t)$ that will be detailed below (Figure 6). In addition, a static threshold S_{80} is used for emergency stop (Figure 6). From these thresholds, three areas can be distinguished and the detection is performed by comparing the online temperature measurements with the dynamical threshold $D_{Limit}(t)$ and $S_{Limit}(t)$. In order to limit the influence of noise, the measured temperature $T_r(t)$ is first filtered by using a Kalman Filter. $f(T_r(t))$ refers to as the filtered temperature at time t .

- Green area: the reaction is in a safe mode when $f(T_r(t))$ is lower than the dynamical threshold $D_{Limit}(t)$. The temperature variations in the green area are assumed to be due to the reaction, the measurement noise and the acceptable disturbances.
- Orange area: the reaction is in a dangerous mode when $f(T_r(t))$ is between the two thresholds $D_{Limit}(t)$ and $S_{Limit}(t)$. The temperature variations are assumed to be due to a fault and an alarm is generated as soon as $f(T_r(t))$ exceeds $D_{Limit}(t)$ for n successive measurements points.

- Red area: the reaction is in a critical mode when $f(T_r(t))$ is between the dynamical threshold $S_{Limit}(t)$ and static threshold S_{80} . A second alarm is generated as soon as $f(T_r(t))$ exceeds $S_{Limit}(t)$.

In addition, the reaction emergency stops if $f(T_r(t))$ exceeds the static threshold S_{80} which is set at 80 °C in order to avoid a runaway reaction due to the thermal decomposition of HP because the decomposition of HP can occur at a temperature higher than 90 °C (Di Serio et al., 2017).

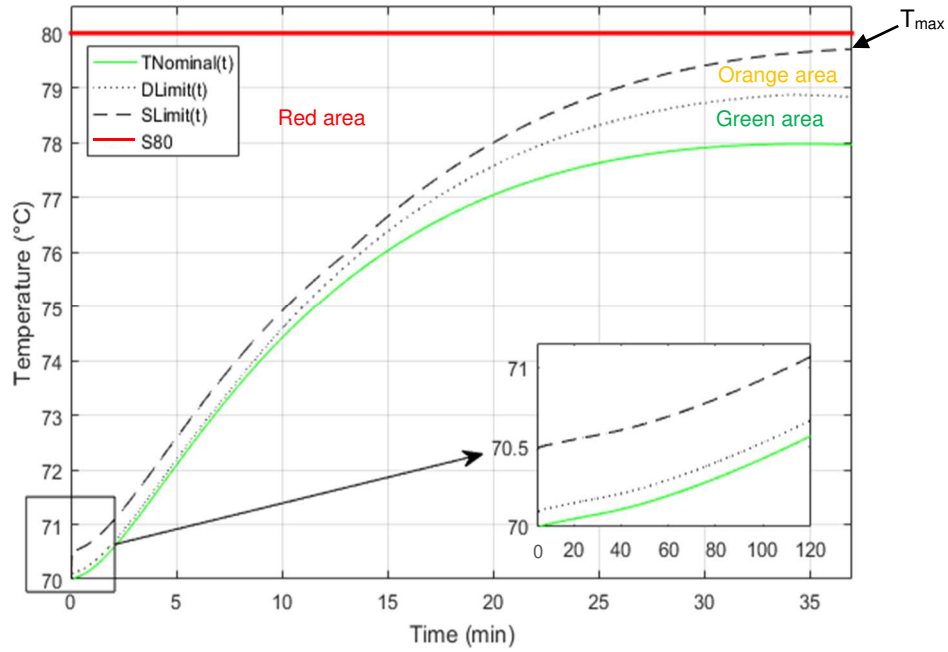


Figure 6. Dynamical thresholds $D_{Limit}(t)$ and $S_{Limit}(t)$ and static threshold S_{80} .

5.2. Decision functions

The decision function for the first alarm is described in Eq (15) and Figure 7.

$$\begin{aligned}
 D_1(t) &= 1 \text{ if } f(T_r(k)) > D_{Limit}(k) \text{ for } k \in \{t-n+1, \dots, t-1, t\} \\
 D_1(t) &= 0 \text{ otherwise}
 \end{aligned} \tag{15}$$

In order to avoid false alarms, $D(t) = 1$ only if the filtered temperature is larger than $D_{Limit}(t)$ for the n successive points $k \in \{t-n+1, \dots, t-1, t\}$ where $n = 10$; $D(t) = 0$, otherwise. The decision function for the second alarm is described in Eq (16).

$$\begin{aligned}
 D_2(t) &= 1 \text{ if } f(T_r(t)) > S_{Limit}(t) \\
 D_2(t) &= 0 \text{ otherwise}
 \end{aligned} \tag{16}$$

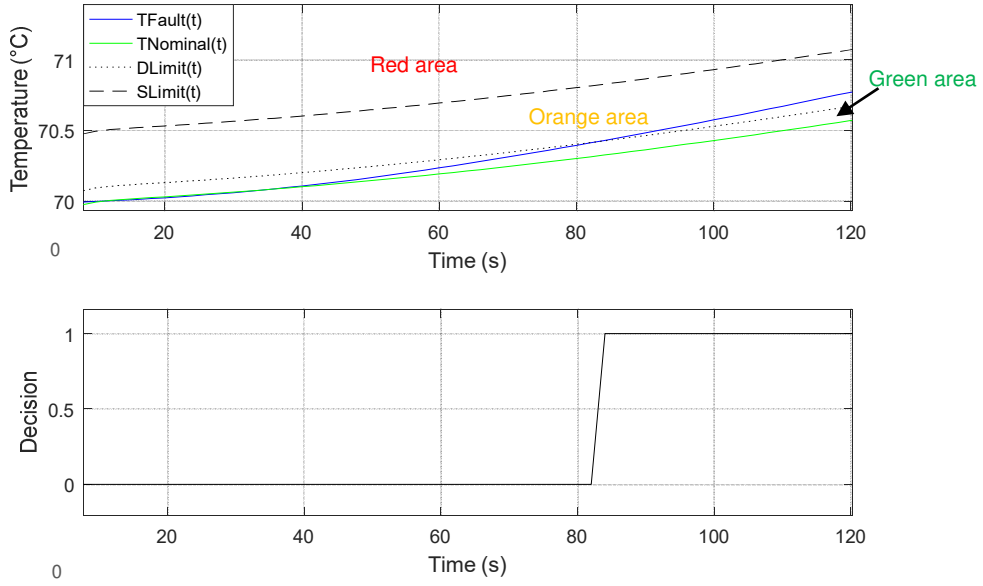


Figure 7. Detection thresholds (top) and decision function (bottom) when a fault occurs

5.3. Detection thresholds computation

The dynamical thresholds $D_{Limit}(t)$ and $S_{Limit}(t)$ have been computed according to the three following principles:

1. An increase of initial concentration of the reagents FA or HP or the presence of impurities accelerates the temperature increase and also increases the maximum value of the temperature reached during the reaction.
2. Sensor noises are taken into consideration and a tolerance margin $M_T = 0.1$ °C is used in order to avoid false alarms due to sensor noises.
3. Only permanent faults are taken into consideration. Multiple faults and intermittent faults are not considered in this work.

The dynamical thresholds $D_{limit}(t)$ and $S_{limit}(t)$ are defined according to Eq. (17) and Eq. (18).

$$D_{Limit}(t) = \max\left(\min\left(T_{FA1}(t), T_{HP1}(t), T_{Cu1}(t), T_{Tj1}(t), T_{Nr1}(t), T_{Qm1}(t)\right), T_{Nominal}(t) + M_T\right) \quad (17)$$

$$S_{Limit}(t) = \max\left(\min\left(T_{FA2}(t), T_{HP2}(t), T_{Cu2}(t), T_{Tj2}(t), T_{Nr2}(t), T_{Qm2}(t)\right), T_{Nominal}(t) + 5.M_T\right) \quad (18)$$

where $T_{Nominal}(t)$ is the reaction temperature profile under the nominal conditions and $T_{x1}(t)$ (resp. $T_{x2}(t)$) represents the temperature reaction profile in presence of a fault of class x and of magnitude $\delta x1$ (resp. $\delta x2$) detailed in Table 6. The magnitude $\delta x1$ (resp. $\delta x2$) is estimated (by simulation) such that the maximum value of the temperature reached during the reaction does not exceed 79°C (resp. 80°C).

In the considered reaction, the security temperature threshold is 80 °C because hydrogen peroxide can decompose at this temperature. With regard to this threshold, a confidence margin of 2 °C has been set. Within this margin, two dynamical detection thresholds have been calculated based on M_T and also takes into account the errors linked to the operating conditions (the concentration of the reagents FA, HP and Cu, the jacket temperature T_j , etc.) and the errors of measurement and modeling. Indeed, the use of “min” operator in Eq. (17) and Eq. (18) reduces the rate of non-detection (by considering the most critical fault at each time sample). The use of “max” operator with the nominal temperature $T_{Nominal}(t)$ plus the marge of tolerance reduces the rate of false alarms.

Table 6. Faults magnitude used to define the dynamical thresholds $D_{Limit}(t)$ and $S_{Limit}(t)$.

δx	δFA	δHP	δCu	δT_j	δN_{tr}	δQ_m
Unit	mol.L ⁻¹	mol.L ⁻¹	mol.L ⁻¹	°C	rpm	kg.s ⁻¹
$D_{Limit}(t)$	0.24	0.26	0.02	0.8	-280	-0.66
$S_{Limit}(t)$	0.46	0.53	0.08	1.7	-360	-0.91

5.4. Diagnosis approach

Fault isolation consists to establish a diagnosis by identifying the most probable fault among a set of fault candidates. The isolation uses (i) temperature measurements collected within the time window W of size K opened at detection time; (ii) a multiset of linear classifiers and binary decision diagrams (BDD) indexed by the time. Each element of this multiset is composed by a set of classifiers structured according to a partial order that is defined in the BDD. The features extracted from the collected measurements within W are ranked according to the nearest (in time) set of classifiers. Figure 8 illustrates the main chart of the fault isolation method.

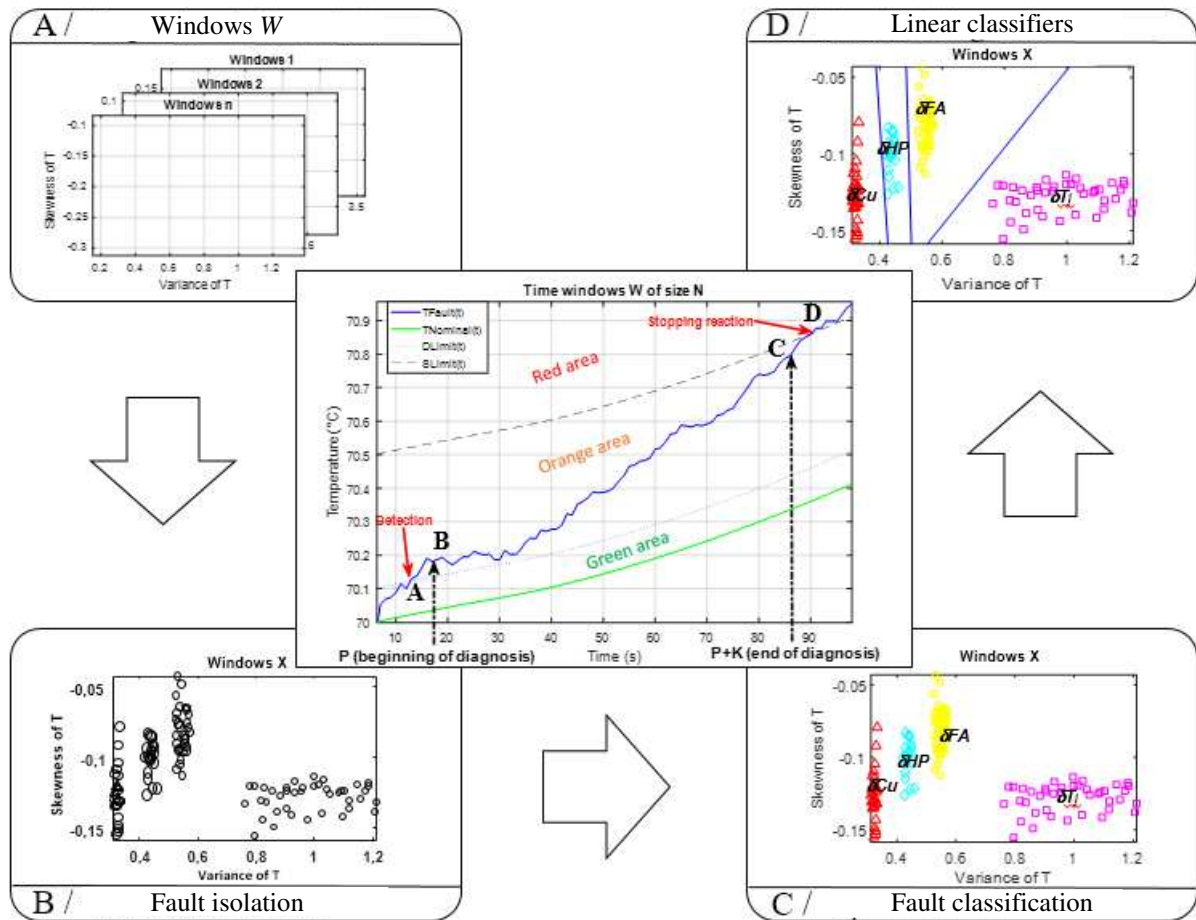


Figure 8. Main chart of the fault isolation method.

As soon as a fault is detected at time p , an acquisition window W is opened to collect the K successive measurements of the temperature $W = \{T(p), T(p + 1), \dots, T(p + K)\}$. The W windows are structured in the database as a function of time (Figure 8-A). The size of the window W is limited by K and by the second threshold $S_{Limit}(t)$. Statistical features (Table 5) will be extracted from the measurements collected within the time window W . The features obtained will be used to perform the fault isolation (Figure 8-B) by using a hierarchical classification method that requires multisets of linear classifiers and binary decision diagrams from a database indexed with the time (the multisets of linear classifiers and binary decision diagrams have been obtained based on simulations under normal and abnormal conditions when faults occur at different times). Depending on the detection time, the multiset of linear classifiers and the binary decision diagram computed for the nearest time will be used. The linear separators of Ho and Kashyap are used to separate and define the location areas of each

fault (Figures 8-C and 8-D). The set of classifiers is structured by the corresponding BDD. The value of parameter K is chosen equal to 300s in order to separate properly the faults.

5.5. Linear classifiers

Linear classifiers are used to linearly separate the extracted features according to the set of fault candidates (Figure 9). According to numerous simulations and experiments, the considered faults are linearly separable in the space of extracted parameters. The main advantages to use linear classifiers, compared to non-linear ones (Barakat et. Al., 2011) is their simplicity. For this purpose, the usual Ho and Kashyap method (Cornuéjols et al., 2018) was iteratively applied to separate 7 classes of data: the nominal class and the 6 faulty modes (Table 3).

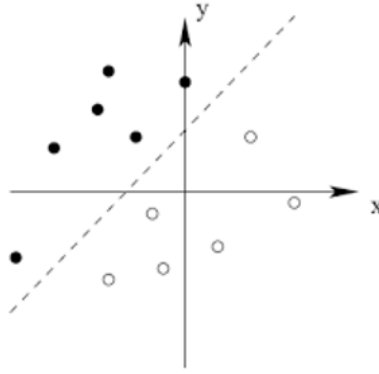


Figure 9. Example of linear separator.

The Ho and Kashyap method is an iterative algorithm that determines if two sets of points are linearly separable, by calculating a sequence of values A_t and B_t from an arbitrary vector B_0 , Eq. (19).

$$A_t^T = B_t^T M^+ \quad (19)$$

where A_t^T is the parameter vector of a linear separator and B_t^T is a vector whose coordinates are positive. M is the matrix grouping the data to be separated and $M^+ = M^T (MM^T)^{-1}$ is the inverse pseudo of M .

Subsequently, the criterion $J(A_t, B_t) = \frac{1}{2} \|A_t^T M - B_t^T\|^2$ must be minimized by calculating the gradient $\nabla_{B_t} J(A_t, B_t)$ of $J(A_t, B_t)$ with respect to B_t , Eq. (20).

$$\nabla_{B_t} J(A_t, B_t) = -(A_t^T M - B_t^T) \quad (20)$$

and deducting a value B_{t+1} such that $J(A_t, B_{t+1}) \leq J(A_t, B_t)$, Eq. (21).

$$B_{t+1}^T = B_t^T + \alpha [A_t^T M - B_t^T] \quad (21)$$

where α is a positive coefficient that adjusts the convergence speed of the algorithm. This procedure converges to a null value of J when the two classes are separable, otherwise it converges to a positive value. The stopping criterion can be $J(A_t, B_t) \approx J(A_{t+1}, B_{t+1})$ or $t \geq t_{max}$. To extend the linear discrimination to 3 or more classes (as it is the case in our application), one use a multi-step hierarchical strategy encoded in a BDD that calculates at each step the linear separator that separates as well as possible the data in two sub-groups of classes.

5.6. Binary decision diagrams (BDD)

In order to perform the classification in an efficient way, BDD have been used to define partial orders within each set of classifiers. A BDD is a tree that represents the connectivity in the dataset in a compact form. A BDD has a single initial node with two successors (i.e. the first linear classifier to be applied) that separates the set of data into two subgroups. Then it has several intermediate nodes, each one with two successors that refine the classification by introducing more subgroups. Finally, it has a set of final nodes without any successor that represent the classes of faults. Each non-terminal node has two successors, one with a bow marked 1 for “true” and the other with a bow marked 0 for “false”. For example, the BDD in Figure 10 separates the 6 classes of faults $\{\delta FA, \delta HP, \delta Cu, \delta I_j, \delta N_{tr}, \delta Q_m\}$ in a 4 steps approach. First the groups of faults $\{\delta FA, \delta HP, \delta Cu, \delta I_j\}$ and $\{\delta N_{tr}, \delta Q_m\}$ are separated. Second, $\{\delta FA, \delta HP, \delta Cu, \delta I_j\}$ is refined in $\{\delta I_j\}$ and a subgroup $\{\delta FA, \delta HP, \delta Cu\}$ and $\{\delta N_{tr}, \delta Q_m\}$ is refined in $\{\delta N_{tr}\}, \{\delta Q_m\}$. Third, $\{\delta FA, \delta HP, \delta Cu\}$ is refined in $\{\delta Cu\}$ and a subgroup $\{\delta FA, \delta HP\}$. Finally, $\{\delta FA, \delta HP\}$ is separated in the two classes of faults $\{\delta FA\}$ and $\{\delta HP\}$. At each step, a unique linear separator is used to separate as well as possible the data in two sub-groups of classes.

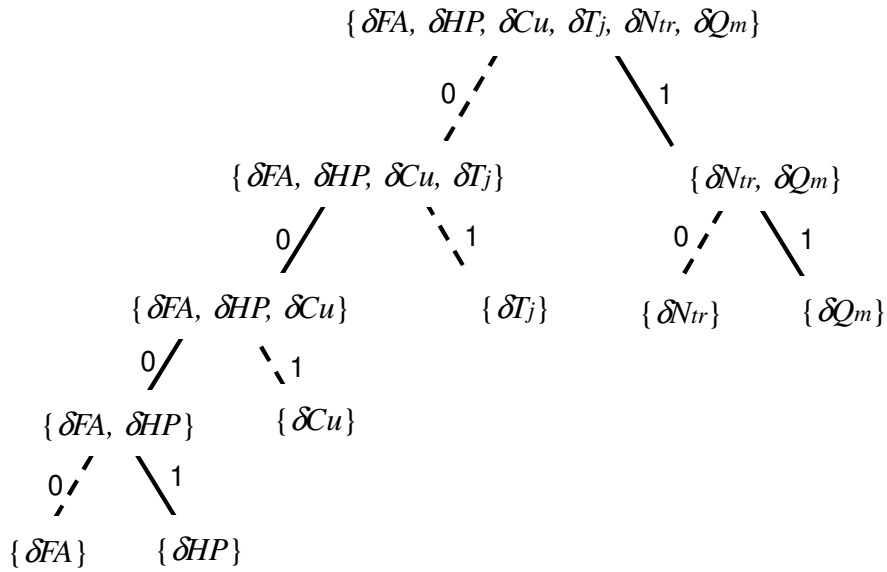


Figure 10. Example of BDD for faults classification.

6. Results and discussion

The proposed detection and diagnosis method has been validated on a set of 210 simulations. These simulations contain scenarios where the six faults previously described occur randomly and also healthy scenarios. A random signal of magnitude $0.1 \text{ } ^\circ\text{C}$ has been added in order to take into account the measurement noise. The value of the tolerance temperature margin is $M_T = 0.1^\circ\text{C}$ and the memory parameter is $n = 10$. The size of the time window is usually $K = 300\text{s}$ whereas the position p depends on the detection time.

6.1. Fault detection

In order to evaluate the performance of the detection method, three indicators are introduced.

- Non-detection rate (*RND*) is the ratio between the number of undetected faults and the number of faults encountered by the system.
- False alarm rate (*RFA*) is the ratio between the number of false alarms and the number of alarms.
- Average detection delay (*ADD*) is the delay between the occurrence of a fault and the detection time.

The results obtained with simulated data lead to $RFA = 0$ and $RND = 0$. ADD are reported in Table 7.

Table 7. Average detection time for the six classes of faults

Fault	δFA	δHP	δCu	δT_j	δN_{tr}	δQ_m
ADD	64 s	80 s	40 s	29 s	354 s	290 s

Early detection is ensured for the faults δFA and δHP affecting the concentration of reagents, the presence of impurities δCu and the increase in cooling temperature system δT_j . However, a larger detection delay is observed for stirring rate fault δN_{tr} and the fault in the flow of heat transfer fluid δQ_m . The weak influence of these two last faults on the reaction system appears especially at the beginning of the reaction when the temperatures T_j and T_r are close. Despite this difficulty, the detection delay remains reasonable compared to the average time to reach the maximum temperature of the reaction (35 min). In particular, the residual time is enough to correct the deviation using online control methods (Vernières-Hassimi and Leveneur, 2015), or setting up preventive actions and security barriers (Misuri et al., 2018).

6.2. Fault diagnosis

The performance of the diagnosis method is evaluated by computing the confusion matrices for a set of 260 simulations (Tables 8, 9 and 10). The rows of the confusion matrix represent the actual membership classes (y) of the data and the columns (x) represent the decisions returned by the classification system. Consequently, the cell C (y, x) gives the percentage of data in class y that are ranked as x by the system.

The diagnosis of early detected faults concerns the faults of type 0 (F1, F2, F3) (i.e. δFA , δHP , δCu) and also the faults of type 1 (F4, F5, F6) (i.e. δT_j , δN_{tr} , δQ_m) when these faults early occur. Figure 11 shows (i) the BDD used to perform the classification; (ii) the set of linear classifiers computed when measurements are collected within the window $W = [30s; 330s]$; (iii) the characteristic points obtained for the considered series of simulations.

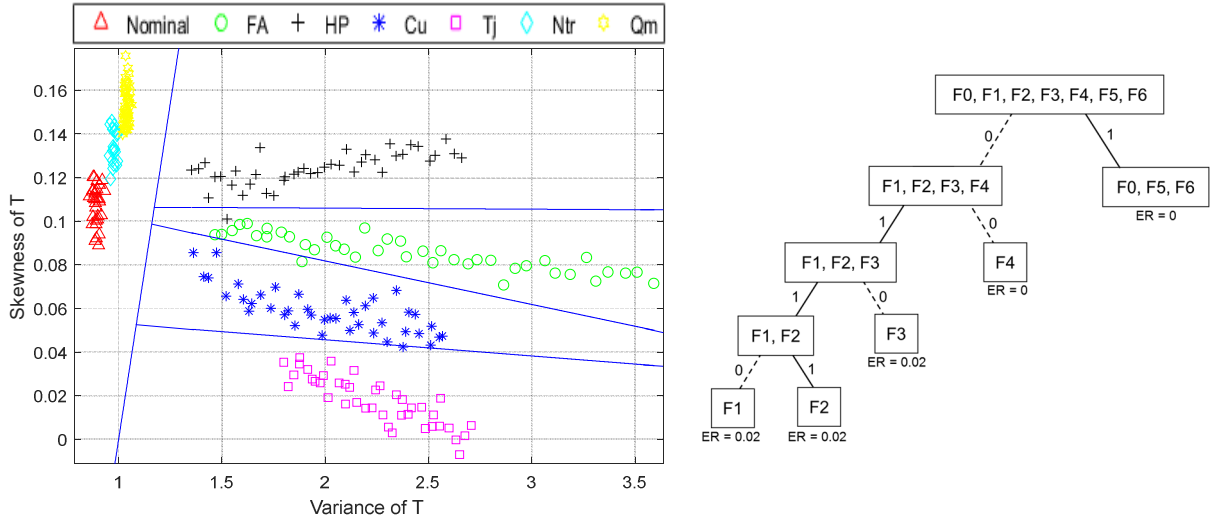


Figure 11. Faults diagnosis for time window $W = [30s : 330s]$.

In the case of diagnosis of early detected faults, four linear classifiers were used to separate the faults F1 to F4 from each other and also to separate them from the group $\{F0, F5$ and $F6\}$, where F0 stands for the nominal fault free situation. Table 8 represents the confusion matrix of the obtained results for the faults F1 to F4.

Table 8. Confusion matrix for early detected faults δFA , δHP , δCu , δT_j with $W = [30s : 330s]$

	δFA	δHP	δCu	δT_j	$\{\delta N_{tr}, \delta Q_m, Nominal\}$
δFA (41 simulations)	40	0	1	0	0
δHP (41 simulations)	1	40	0	0	0
δCu (41 simulations)	0	0	40	1	0
δT_j (41 simulations)	0	0	0	41	0
$\{\delta N_{tr}, \delta Q_m, Nominal\}$ (96 simulations)	0	0	0	0	96

The performance of this classifier shows that 40 faults of δFA , δHP and δCu out of 41 faults are correctly isolated. A few decisions are wrong but these classification errors can be corrected by increasing the size of the window W . Note that the faults δN_{tr} and δQ_m cannot be isolated with this diagnoser when they early occur. To isolate these faults, it is necessary to move the measurement window $W = [150s : 450s]$. Figure 12 shows the classification results for this new window

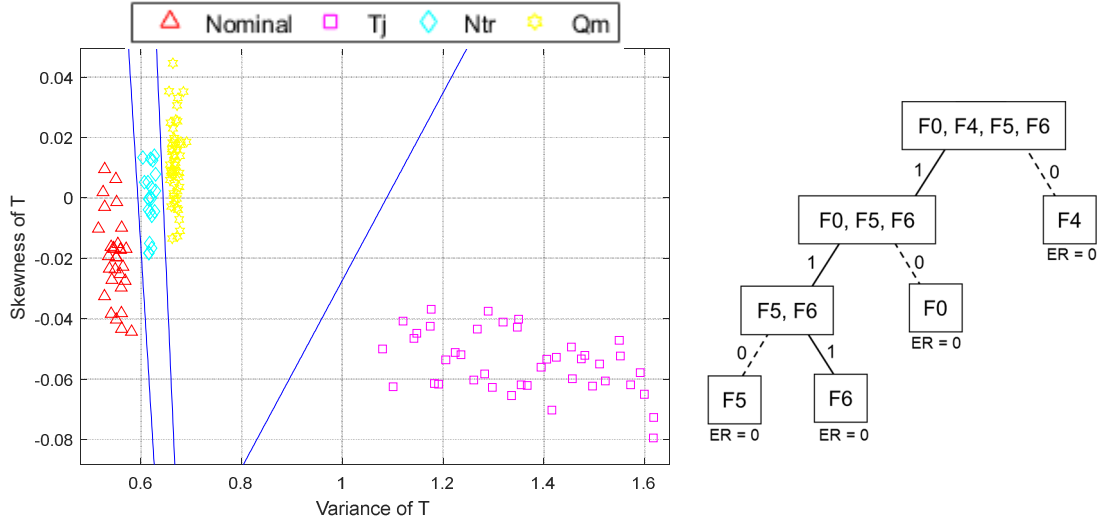


Figure 12. Faults diagnosis for time window $W = [150s : 450s]$.

In this time window, three linear classifiers were used to separate the faults F0, F4, F5 and F6. In our set of simulations, the performance is shown in Table 9, but one should take care that the relative close position of the different groups of data $\{\delta N_{tr}, \delta Q_m, \text{Nominal}\}$ prevents the use of this diagnoser if the magnitude of noise increases.

Table 9. Confusion matrix for early detected faults δN_{tr} , δQ_m , δT_j with $W = [150s : 450s]$

	<i>Nominal</i>	δT_j	δN_{tr}	δQ_m
<i>Nominal</i> (28 simulations)	28	0	0	0
δT_j (41 simulations)	0	41	0	0
δN_{tr} (20 simulations)	0	0	20	0
δQ_m (48 simulations)	0	0	0	48

The faults δN_{tr} , δQ_m and δT_j may occur at any time and in particular late after the starting of the reaction. The time when the faults occur changes the characteristics of the group of data in plan (variance, skewness). For this reason, it becomes necessary to use a multiset of linear classifiers and BDD where the classifiers and BDD are indexed by the time. As an example, Figure 13 shows the classification of faults for the time window $W = [450s : 750s]$.

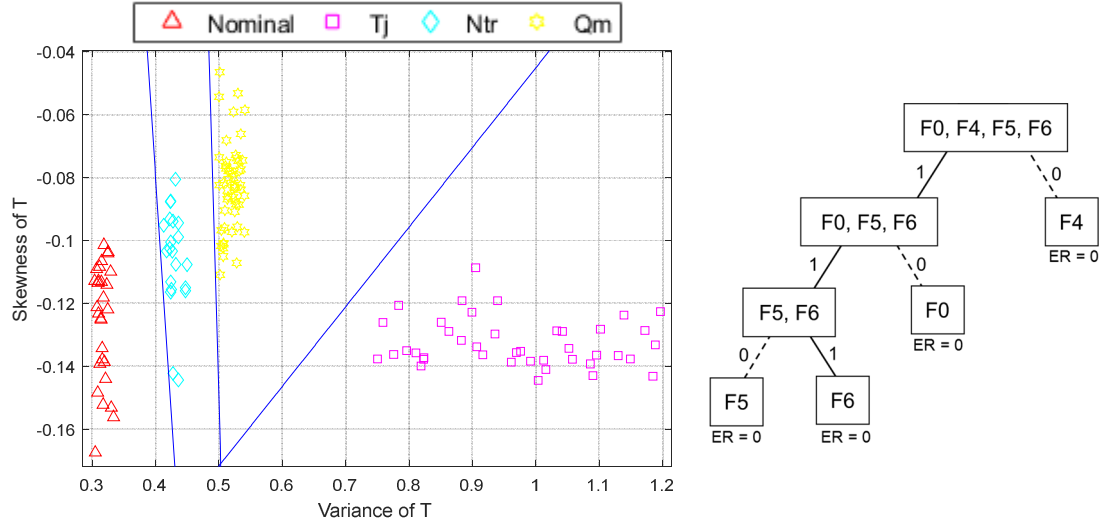


Figure 13. Faults diagnosis for time window $W = [450s : 750s]$.

Also in this case, three linear classifiers were used to separate the fault F0, F4, F5 and F6. the performance for the considered set of simulations is shown in Table 10.

Table 10. Confusion matrix for late detected faults δN_{tr} , δQ_m and δT_j with $W = [450s : 750s]$

	<i>Nominal</i>	δT_j	δN_{tr}	δQ_m
<i>Nominal</i> (28 simulations)	28	0	0	0
δT_j (41 simulations)	0	41	0	0
δN_{tr} (20 simulations)	0	0	20	0
δQ_m (48 simulations)	0	0	0	48

In general, for the diagnosis of early detected faults (initial windows time), four linear classifiers were used to separate the different faults. For the others time windows three linear classifiers were used for each windows.

6.3. Experimental validation

Experimental validations of the proposed faults detection and diagnosis method are also performed. A set of 27 experiments under abnormal conditions are carried out in the RC1 batch reactor. Table 10 shows the results. Note that fault F6 (i.e. δQ_m) could not be tested for safety reasons. The detection results for the faults δFA , δHP , δCu and δT_j were as good as expected. The detection delay varies between 24s and 126s. The fault δN_{tr} was also detected but an important delay should be noticed when the stirring rate decreases from 400 rpm to 100

or 50 rpm. When the stirring rate decreases from 400 to 200 rpm, then the fault δN_{tr} becomes undetectable because of the relative weak sensitivity of the overall heat exchange coefficient with respect to the variation of the stirring rate (Figure 14). Overall, the performance of the fault detection method is RND = 11%, RFA = 0% and ADD = 111s for experimental data.

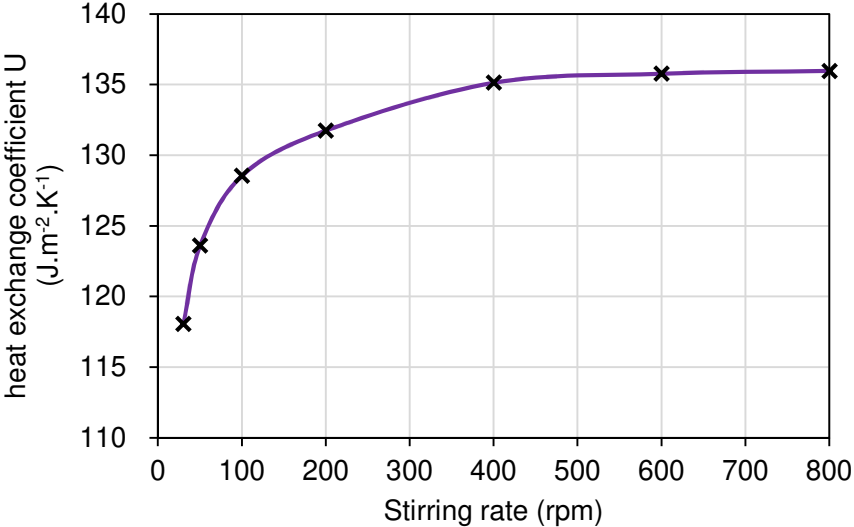


Figure 14. Sensitivity of the heat exchange coefficient with respect to the stirring rate.

The diagnosis results are also presented in Table 11. Each detected fault was well classified, excepted the undetected fault δN_{tr} . By calculating the classification rate for the 27 experiments, a classification rate of 89% was found. Note that the performance reported in Section 6.3 reflects only the experimental validation and that this performance is not as good as the performance obtained with simulation data and reported in the previous section.

Table 11. Faults detection and diagnosis results for experimental data (X means the fault is not detected; ∞ means that the abnormal temperature profile does not reach the thresholds)

Fault	Symbol	Normal condition	Abnormal condition	Date of fault (s)	Detection delay (s)	Diagnosis result	Diagnosis duration (s)	Duration to reach $S_{Limit}(t)$ (s)	Duration to reach S_{80} (s)
F1	δFA	2.5 mol.L ⁻¹	3.01 mol.L ⁻¹	Initial	106	FA	[30s 330s]	136	1230
			3.51 mol.L ⁻¹		46	FA	[30s 330s]	96	766
			4.08 mol.L ⁻¹		76	FA	[30s 330s]	50	546
F2	δHP	2.8 mol.L ⁻¹	3.52 mol.L ⁻¹	Initial	126	HP	[30s 330s]	144	1090
			4.05 mol.L ⁻¹		74	HP	[30s 330s]	104	774
			4.55 mol.L ⁻¹		56	HP	[30s 330s]	86	620
F3	δCu	0 mol.L ⁻¹	0.01 mol.L ⁻¹	Initial	42	Cu	[30s 330s]	160	1360
			0.03 mol.L ⁻¹		52	Cu	[30s 330s]	92	904
			0.06 mol.L ⁻¹		38	Cu	[30s 330s]	84	838
F4	δT_j	70 °C	72 °C	Initial	24	T_j	[30s 330s]	126	1276
				300	66	T_j	[350s 650s]	112	1118
				600	94	T_j	[650s 950s]	26	714
			74 °C	Initial	38	T_j	[30s 330s]	62	834
				300	56	T_j	[350s 650s]	52	666
				600	70	T_j	[650s 950s]	20	530
			76 °C	Initial	42	T_j	[30s 330s]	42	686
				300	64	T_j	[350s 650s]	36	589
				600	64	T_j	[650s 950s]	16	376
F5	δN_{tr}	400 rpm	200 rpm	Initial	X	X	X	X	X
				300	X	X	X	X	X
				600	X	X	X	X	X
			100 rpm	Initial	324	N_{tr}	[350s 650s]	2278	∞
				300	166	N_{tr}	[450s 750s]	∞	∞
				600	370	N_{tr}	[950s 1250s]	∞	∞
			50 rpm	Initial	396	N_{tr}	[350s 650s]	1922	∞
				300	180	N_{tr}	[450s 750s]	496	∞
				600	394	N_{tr}	[950s 1250s]	1382	∞

7. Conclusions

The purpose of this paper was to propose an online fault detection and diagnosis approach in order to prevent thermal runaway reactions. A set of six different faults classes due to operator errors has been considered. The method was validated by simulation and experiments for an exothermic reaction of perhydrolysis of formic acid in a batch reactor.

The main advantages of the proposed method can be summed up. An early and robust faults detection was performed thanks the use of a double dynamical threshold. Detection performance has been proved excepted for the degraded modes of the agitator that affect weakly and slowly the reaction. An efficient diagnosis schema was also proposed based on the combined use of a multiset of classifiers and BDD that are both indexed by the time. The detection time was used to select properly the set of adequate classifiers. These classifiers have proved a high isolability rate (excepted for faults affecting the agitator).

The main limitation of the proposed approach lies on the necessity to use an accurate model of the considered reaction. Such a model is mandatory not only to generate the expected temperature variation but also to emulate the effects of the considered faults in order to design the set of linear classifiers and BDD used for isolation issues.

Our further works are to adapt the proposed approach for semi-batch and open reactors, in order to address practical detection and diagnosis problems in industrial environment.

Acknowledgments

This project AMED has been funded with the support from the European Union with the European Regional Development Fund (ERDF) and from the Regional Council of Normandie.

References

- Adler, J., Enig, J.W., 1964. The critical conditions in thermal explosion theory with reactant consumption. *Combust. Flame* 8, 97–103. [https://doi.org/10.1016/0010-2180\(64\)90035-5](https://doi.org/10.1016/0010-2180(64)90035-5)
- Alcala, C.F., Dunia, R., Qin, S.J., 2012. Monitoring of Dynamic Processes with Subspace Identification and Principal Component Analysis. *IFAC Proceedings Volumes*, 8th IFAC Symposium on Fault Detection, Supervision and Safety of Technical Processes 45, 684–689. <https://doi.org/10.3182/20120829-3-MX-2028.00238>

- Ammiche, M., Kouadri, A., Bensmail, A., 2018. A Modified Moving Window dynamic PCA with Fuzzy Logic Filter and application to fault detection. *Chemometrics and Intelligent Laboratory Systems* 177, 100–113. <https://doi.org/10.1016/j.chemolab.2018.04.012>
- Balasubramanian, S.G., Louvar, J.F., 2002. Study of major accidents and lessons learned. *Proc. Safety Prog.* 21, 237–244. <https://doi.org/10.1002/prs.680210309>
- Ballesteros-Moncada, H., Herrera-López, E.J., Anzures-Marín, J., 2015. Fuzzy model-based observers for fault detection in CSTR. *ISA Transactions* 59, 325–333. <https://doi.org/10.1016/j.isatra.2015.10.006>
- Barakat M., Druaux F., Lefebvre D., Khalil M., Mustapha M., Self Adaptive Growing Neural Network classifier for Faults Detection and Diagnosis, *Neurocomputing*, Vol. 74, Issue 18, Pages 3865-3876, November 2011
- Basseville, M., Nikiforov, I., 1993. *Detection of Abrupt Changes: Theory and Applications*. Englewood Cliffs: NJ: Prentice-Hall.
- Benkouider, A.M., Buvat, J.C., Cosmao, J.M., Saboni, A., 2009. Fault detection in semi-batch reactor using the EKF and statistical method. *Journal of Loss Prevention in the Process Industries* 22, 153–161. <https://doi.org/10.1016/j.jlp.2008.11.006>
- Benkouider, A.M., Kessas, R., Yahiaoui, A., Buvat, J.C., Guella, S., 2012. A hybrid approach to faults detection and diagnosis in batch and semi-batch reactors by using EKF and neural network classifier. *Journal of Loss Prevention in the Process Industries* 25, 694–702. <https://doi.org/10.1016/j.jlp.2012.03.005>
- Bin Shams, M.A., Budman, H.M., Duever, T.A., 2011. Fault detection, identification and diagnosis using CUSUM based PCA. *Chemical Engineering Science* 66, 4488–4498. <https://doi.org/10.1016/j.ces.2011.05.028>
- Bosch, J., Strozzi, F., Snee, T.J., Hare, J.A., Zaldívar, J.M., 2004. A comparative analysis between temperature and pressure measurements for early detection of runaway initiation. *J. Loss Prev. Process Ind.* 17, 389–395. <https://doi.org/10.1016/j.jlp.2004.07.003>
- Bowes P.C., 1984. *Self-Heating: Evaluating and Controlling the Hazard*, HMSO Books, London
- Bryce, G., Gaudard, M., Joiner, B., 1997. Estimating the Standard Deviation for Individuals Control Charts. *Quality Engineering*, 10(2), 331-341. <https://doi.org/10.1080/08982119708919139>
- Campanella, A., Fontanini, C., Baltanás, M.A., 2008. High yield epoxidation of fatty acid methyl esters with performic acid generated in situ. *Chemical Engineering Journal* 144, 466–475. <https://doi.org/10.1016/j.cej.2008.07.016>
- Chang, S.Y., Lin, C.R., Chang, C.-T., Yu, S.W., 2001. On-Line Fault Diagnosis Using Dynamic Fault Tree. *IFAC Proceedings Volumes*, 4th IFAC Workshop on On-Line Fault Detection and Supervision in the Chemical Process Industries 2001, Jeju Island, Korea, 7-8 June 2001 34, 167–172. [https://doi.org/10.1016/S1474-6670\(17\)33586-3](https://doi.org/10.1016/S1474-6670(17)33586-3)
- Chen, G., Chui, C.K., 1991. A modified adaptive Kalman filter for real-time applications. *IEEE Transactions on Aerospace and Electronic Systems* 27, 149–154. <https://doi.org/10.1109/7.68157>
- Cilliers, A.C., 2013. Benchmarking an expert fault detection and diagnosis system on the Three Mile Island accident event sequence. *Annals of Nuclear Energy* 62, 326–332. <https://doi.org/10.1016/j.anucene.2013.06.037>
- Cornuéjols, A., Miclet, L., Barra, V., 2018. *Apprentissage artificiel: Deep learning, concepts et algorithmes*. Editions Eyrolles.
- Costa, A., Rahim, M., 2006. The non-central chi-square chart with two-stage samplings. *European Journal of Operational Research*, 171, 64-73. <https://doi.org/10.1016/j.ejor.2004.09.027>

- Crowder, S. V., 1987. Run-Length Distributions of EWMA Charts. *Technometrics*(29), 401-407. <https://doi.org/10.1080/00401706.1987.10488267>
- Dakkoune, A., Vernières-Hassimi, L., Leveneur, S., Lefebvre, D., Estel, L., 2018a. Risk analysis of French chemical industry. *Safety Science* 105, 77–85. <https://doi.org/10.1016/j.ssci.2018.02.003>
- Dakkoune, A., Vernières-Hassimi, L., Leveneur, S., Lefebvre, D., Estel, L., 2018b. Fault Detection in the Green Chemical Process: Application to an Exothermic Reaction. 1 67, 43–48. <https://doi.org/10.3303/CET1867008>
- Dakkoune, A., Vernières-Hassimi, L., Leveneur, S., Lefebvre, D., Estel, L., 2019. Analysis of thermal runaway events in French chemical industry. *J. Loss Prev. Process Ind.* 62, 103938. <https://doi.org/10.1016/j.jlp.2019.103938>
- Di Maio, F., Bandini, A., Damato, M., Zio, E., 2018. A Regional Sensitivity Analysis-based Expert System for safety margins control. *Nuclear Engineering and Design* 330, 400–408. <https://doi.org/10.1016/j.nucengdes.2018.01.002>
- Di Serio, M., Russo, V., Santacesaria, E., Tesser, R., Turco, R., Vitiello, R., 2017. Liquid–Liquid–Solid Model for the Epoxidation of Soybean Oil Catalyzed by Amberlyst-16. *Ind. Eng. Chem. Res.* 56, 12963–12971. <https://doi.org/10.1021/acs.iecr.7b00881>
- Dream, R. F. 1999. Heat transfer in agitated jacketed vessels. *Chemical Engineering*, 90–96.
- Du, Y., Du, D., 2018. Fault detection and diagnosis using empirical mode decomposition based principal component analysis. *Computers & Chemical Engineering* 115, 1–21. <https://doi.org/10.1016/j.compchemeng.2018.03.022>
- Fadda, G., Chebeir, J., Salas, S.D., Romagnoli, J.A., 2019. Joint dynamic data reconciliation/parameter estimation: Application to an industrial pyrolysis reactor. *Applied Thermal Engineering* 158, 113726. <https://doi.org/10.1016/j.applthermaleng.2019.113726>
- Fezai, R., Mansouri, M., Taouali, O., Harkat, M.F., Bouguila, N., 2018. Online reduced kernel principal component analysis for process monitoring. *Journal of Process Control* 61, 1–11. <https://doi.org/10.1016/j.jprocont.2017.10.010>
- Filippis, P.D., Scarsella, M., Verdone, N., 2009. Peroxyformic Acid Formation: A Kinetic Study. *Ind. Eng. Chem. Res.* 48, 1372–1375. <https://doi.org/10.1021/ie801163j>
- Francis, R., Bekera, B., 2014. A metric and frameworks for resilience analysis of engineered and infrastructure systems. *Reliab. Eng. Syst. Saf.* 121, 90–103. <https://doi.org/10.1016/j.res.2013.07.004>
- Frank, P.M., 1990. Fault diagnosis in dynamic systems using analytical and knowledge-based redundancy: A survey and some new results. *Automatica* 26, 459–474. [https://doi.org/10.1016/0005-1098\(90\)90018-D](https://doi.org/10.1016/0005-1098(90)90018-D)
- Frank, P.M., Ding, X., 1997. Survey of robust residual generation and evaluation methods in observer-based fault detection systems. *Journal of Process Control* 7, 403–424. [https://doi.org/10.1016/S0959-1524\(97\)00016-4](https://doi.org/10.1016/S0959-1524(97)00016-4)
- Gelb, A. 1974. *Applied Optimal Estimation*. The M.I.T. Press
- Gertler, J., Singer, D., 1990. A new structural framework for parity equation-based failure detection and isolation. *Automatica* 26, 381–388. [https://doi.org/10.1016/0005-1098\(90\)90133-3](https://doi.org/10.1016/0005-1098(90)90133-3)
- Guo, Z.-C., Bai, W.-S., Chen, Y.-J., Wang, R., Hao, L., Wei, H.-Y., 2016. An adiabatic criterion for runaway detection in semibatch reactors. *Chem. Eng. J.* 288, 50–58. <https://doi.org/10.1016/j.cej.2015.11.065>
- Harkat, M.-F., Mansouri, M., Nounou, M., Nounou, H., 2019. Fault detection of uncertain nonlinear process using interval-valued data-driven approach. *Chemical Engineering Science* 205, 36–45. <https://doi.org/10.1016/j.ces.2018.11.063>

- Hub, L., Jones, J.D., 1986. Early on-line detection of exothermic reactions. *Plant/Operations Prog.* 5, 221–224. <https://doi.org/10.1002/prsb.720050408>
- Isermann, R., 2006. *Fault-Diagnosis Systems: An Introduction from Fault Detection to Fault Tolerance*. Springer Science & Business Media.
- Jain, P., Pasman, H.J., Waldram, S., Pistikopoulos, E.N., Mannan, M.S., 2018. Process Resilience Analysis Framework (PRAF): A systems approach for improved risk and safety management. *J. Loss Prev. Process Ind., Risk Analysis in Process Industries: State-of-the-art and the Future* 53, 61–73. <https://doi.org/10.1016/j.jlp.2017.08.006>
- Jain, P., Pistikopoulos, E.N., Mannan, M.S., 2019. Process resilience analysis based data-driven maintenance optimization: Application to cooling tower operations. *Comput. Chem. Eng.* 121, 27–45. <https://doi.org/10.1016/j.compchemeng.2018.10.019>
- Jazwinski, A. H., 1970. *Stochastic Process and Filtrng Theory*, vol. 64 of *Mathematics in Science and Engineering*. Academic Press, In
- Jia, F., Martin, E.B., Morris, A.J., 2000. Non-linear principal components analysis with application to process fault detection. *International Journal of Systems Science* 31, 1473–1487. <https://doi.org/10.1080/00207720050197848>
- Kabbaj, N., Doncescu, A., Aguilar-Martin, J., 2009. Parity Relations based on elimination theory for Fault Detection in a bioprocess. *IFAC Proceedings Volumes, 7th IFAC Symposium on Fault Detection, Supervision and Safety of Technical Processes* 42, 1270–1275. <https://doi.org/10.3182/20090630-4-ES-2003.00208>
- Kohcielnny, J.M., 1999. Application of Fuzzy Logic for Fault Isolation in a Three-Tank System. *IFAC Proceedings Volumes, 14th IFAC World Congress 1999, Beijing, Chia, 5-9 July* 32, 7754–7759. [https://doi.org/10.1016/S1474-6670\(17\)57323-1](https://doi.org/10.1016/S1474-6670(17)57323-1)
- Lee, J.-M., Yoo, C., Choi, S.W., Vanrolleghem, P.A., Lee, I.-B., 2004. Nonlinear process monitoring using kernel principal component analysis. *Chemical Engineering Science* 59, 223–234. <https://doi.org/10.1016/j.ces.2003.09.012>
- Leveneur, S., Thönes, M., Hébert, J.-P., Taouk, B., Salmi, T., 2012. From Kinetic Study to Thermal Safety Assessment: Application to Peroxyformic Acid Synthesis. *Ind. Eng. Chem. Res.* 51, 13999–14007. <https://doi.org/10.1021/ie3017847>
- Lucas, J. M., Crosier, R. B., 1982. Robust CUSUM: A Robustness Study for CUSUM Quality Control Schemes. *Communications in Statistics, A* 11, 2669-2687. <https://doi.org/10.1080/03610928208828414>
- Lucas, J. M., Saccucci, M. S., 1990. Exponentially Weighted Moving Average Control Schemes: Properties and Enhancements. *Technometrics*(32), 1-29. <https://doi.org/10.1080/00401706.1990.10484583>
- Marco, E., Peña, J.A., Santamaría, J., 1997. Early detection of runaway reactions in systems with gas evolution using on-line mass spectrometry. *Chem. Eng. Sci.* 52, 3107–3115. [https://doi.org/10.1016/S0009-2509\(97\)00120-6](https://doi.org/10.1016/S0009-2509(97)00120-6)
- Miljković, D., 2011. Fault detection methods: A literature survey, in: *2011 Proceedings of the 34th International Convention MIPRO*. Presented at the 2011 Proceedings of the 34th International Convention MIPRO, pp. 750–755.
- Misuri, A., Khakzad, N., Reniers, G., Cozzani, V., 2018. A Bayesian network methodology for optimal security management of critical infrastructures. *Reliability Engineering & System Safety*. <https://doi.org/10.1016/j.ress.2018.03.028>
- Olivier-Maget, N., Hétreux, G., Le Lann, J.M., Le Lann, M.V., 2009. Model-based fault diagnosis for hybrid systems: Application on chemical processes. *Computers & Chemical Engineering, Selected Papers from the 18th European Symposium on Computer Aided Process Engineering (ESCAPE-18)* 33, 1617–1630. <https://doi.org/10.1016/j.compchemeng.2009.04.016>

- Othman, M.R., Ali, M.W., Kamsah, M.Z., 2012. Process Fault Detection Using Hierarchical Artificial Neural Network Diagnosis Strategy. *Jurnal Teknologi* 46, 11–26. <https://doi.org/10.11113/jt.v46.301>
- Page, E. S., 1954. Continuous Inspection Schemes. *Biometrika*, Vol. 41(1/2),100-115.
- Perez-Benito, J.F., 2001. Copper(II)-Catalyzed Decomposition of Hydrogen Peroxide: Catalyst Activation by Halide Ions. *Monatshefte für Chemie* 132, 1477–1492. <https://doi.org/10.1007/s00706017000>
- Pierri, F., Paviglianiti, G., Caccavale, F., Mattei, M., 2008. Observer-based sensor fault detection and isolation for chemical batch reactors. *Engineering Applications of Artificial Intelligence* 21, 1204–1216. <https://doi.org/10.1016/j.engappai.2008.02.002>
- Quantrille, T.E., Liu, Y.A., 2012. *Artificial Intelligence in Chemical Engineering*. Elsevier.
- Ramesh, T.S., Davis, J.F., Schwenzer, G.M., 1992. Knowledge-based diagnosis systems for continuous process operations based upon the task framework. *Computers & Chemical Engineering, An International Journal of Computer Applications in Chemical Engineering* 16, 109–127. [https://doi.org/10.1016/0098-1354\(92\)80009-X](https://doi.org/10.1016/0098-1354(92)80009-X)
- Rich, S.H., Venkatasubramanian, V., Nasrallah, M., Matteo, C., 1989. Development of a diagnosis expert system for a whipped toppings process. *Journal of Loss Prevention in the Process Industries* 2, 145–154. [https://doi.org/10.1016/0950-4230\(89\)80019-1](https://doi.org/10.1016/0950-4230(89)80019-1)
- Roberts, S. W., 1959. Control Chart Tests Based on Geometric Moving Averages. *Technometrics*, 1(3), 239-250. <https://doi.org/10.1080/00401706.1959.10489860>
- Saada, R., Patel, D., Saha, B., 2015. Causes and consequences of thermal runaway incidents—Will they ever be avoided? *Process Safety and Environmental Protection, Bhopal 30th Anniversary* 97, 109–115. <https://doi.org/10.1016/j.psep.2015.02.005>
- Semenov, N., 1928. Zur Theorie des Verbrennungsprozesses. *Z. Für Phys.* 48, 571–582. <https://doi.org/10.1007/BF01340021>
- Shewhart, W. A., 1925. The Application of Statistics as an Aid in Maintaining Quality of a Manufactured Product. *Journal of the American Statistical Association*, 20(152), 546-548. <https://doi.org/10.1080/01621459.1925.10502930>
- Stoessel, F., 2008. *Thermal Safety of Chemical Processes: Risk Assessment and Process Design*. John Wiley & Sons.
- Strozzi, F., Zaldívar, J.M., 1994. A general method for assessing the thermal stability of batch chemical reactors by sensitivity calculation based on Lyapunov exponents. *Chem. Eng. Sci.* 49, 2681–2688. [https://doi.org/10.1016/0009-2509\(94\)E0067-Z](https://doi.org/10.1016/0009-2509(94)E0067-Z)
- Strozzi, F., Zaldívar, J.M., Kronberg, A.E., Westerterp, K.R., 1999. On-Line runaway detection in batch reactors using chaos theory techniques. *AIChE J.* 45, 2429–2443. <https://doi.org/10.1002/aic.690451116>
- Subramanian, S., Ghose, F., Natarajan, P., 2014. Fault Diagnosis of Batch Reactor Using Machine Learning Methods [WWW Document]. *Model. Simul. Eng.* <https://doi.org/10.1155/2014/426402>
- Sun, X., Zhao, X., Du, W., Liu, D., 2011. Kinetics of Formic Acid-autocatalyzed Preparation of Performic Acid in Aqueous Phase. *Chinese Journal of Chemical Engineering* 19, 964–971. [https://doi.org/10.1016/S1004-9541\(11\)60078-5](https://doi.org/10.1016/S1004-9541(11)60078-5)
- Trambouze, P., Euzen, J.-P., 2002. *Les réacteurs chimiques ; de la conception à la mise en oeuvre*. Ed. Technip, Paris.
- Thürlimann, C.M., Villegz, K., 2017. Input estimation as a qualitative trend analysis problem. *Computers & Chemical Engineering, In honor of Professor Rafiqul Gani* 107, 333–342. <https://doi.org/10.1016/j.compchemeng.2017.04.011>
- Ubrich, O., Srinivasan, B., Lerena, P., Bonvin, D., Stoessel, F., 2001. The use of calorimetry for on-line optimisation of isothermal semi-batch reactors. *Chemical Engineering Science* 56, 5147–5156. [https://doi.org/10.1016/S0009-2509\(01\)00183-X](https://doi.org/10.1016/S0009-2509(01)00183-X)

- Vernieres-Hassimi, L., Abdelghani-Idrissi, A., Seguin, D., and Mouhab, N., 2012. Unsteady state maximum temperature estimation and localization in a tubular chemical reactor, *Int. J. Chem. Reactor. Eng.*, 10(1), 1542–6580. <https://doi.org/10.1515/1542-6580.2572>
- Vernières-Hassimi, L., Leveneur, S., 2015. Alternative method to prevent thermal runaway in case of error on operating conditions continuous reactor. *Process Safety and Environmental Protection* 98, 365–373. <https://doi.org/10.1016/j.psep.2015.09.012>
- Vernieres-Hassimi, L., Seguin, D., Abdelghani-Idrissi, M.A., Mouhab, N., 2015. Estimation and Localization of Maximum Temperature in a Tubular Chemical Reactor by Luenberger State Observer. *Chemical Engineering Communications* 202, 70–77. <https://doi.org/10.1080/00986445.2013.828609>
- Vernieres-Hassimi, L., Seguin, D., Abdelghani-Idrissi, M.A., Mouhab, N., 2015. Estimation and Localization of Maximum Temperature in a Tubular Chemical Reactor by Luenberger State Observer. *Chemical Engineering Communications* 202, 70–77. <https://doi.org/10.1080/00986445.2013.828609>
- Wang, X., Zhang, H., Wang, Z., Jiang, B., 1997. In situ epoxidation of ethylene propylene diene rubber by performic acid. *Polymer* 38, 5407–5410. [https://doi.org/10.1016/S0032-3861\(97\)00043-8](https://doi.org/10.1016/S0032-3861(97)00043-8)
- Westerterp, K.R., Molga, E.J., 2006. Safety and Runaway Prevention in Batch and Semibatch Reactors—A Review. *Chemical Engineering Research and Design*, In Honour of Professor Ryszard Pohorecki on the Occasion of his 70th Birthday 84, 543–552. <https://doi.org/10.1205/cherd.05221>
- Zaldívar, J.-M., Bosch, J., Strozzi, F., Zbilut, J.P., 2005. Early warning detection of runaway initiation using non-linear approaches. *Commun. Nonlinear Sci. Numer. Simul.* 10, 299–311. <https://doi.org/10.1016/j.cnsns.2003.08.001>
- Zhang, J., 2008. Batch-to-batch optimal control of a batch polymerisation process based on stacked neural network models. *Chemical Engineering Science, Control of Particulate Processes* 63, 1273–1281. <https://doi.org/10.1016/j.ces.2007.07.047>
- Zhao, H., 2018. Neural component analysis for fault detection. *Chemometrics and Intelligent Laboratory Systems* 176, 11–21. <https://doi.org/10.1016/j.chemolab.2018.02.001>
- Zheng, J.L., Wärnå, J., Salmi, T., Burel, F., Taouk, B., Leveneur, S., 2016. Kinetic modeling strategy for an exothermic multiphase reactor system: Application to vegetable oils epoxidation using Prileschajew method. *AIChE J.* 62, 726–741. <https://doi.org/10.1002/aic.15037>
- Zhou, B., Ye, H., 2016. A study of polynomial fit-based methods for qualitative trend analysis. *Journal of Process Control* 37, 21–33. <https://doi.org/10.1016/j.jprocont.2015.11.003>